

Article

Suitability Assessment Method of Red Tourism Development Using Geospatial and Social Humanity Data: A Case Study of Ruijin City, East China

Yaozu Qin ^{1,2,*}, Li Cao ^{3,*}, Wenjing Li ², Ali Darvishi Bolorani ⁴, Yuan Li ², Xinxin Ke ², Masoud Soleimani ⁴, Qian Yu ² and Cuimin Zhou ²

¹ The Key Laboratory of Digital Land and Resources, East China University of Technology, Nanchang 330013, China

² Faculty of Earth Sciences, East China University of Technology, Nanchang 330013, China; 2020110085@ecut.cn (W.L.); 2020110084@ecut.edu.cn (Y.L.); 2020120009@ecut.edu.cn (X.K.); jiangxi_shangrao@sina.cn (Q.Y.); 2020110012@ecut.edu.cn (C.Z.)

³ Key Laboratory of Natural Resources Monitoring and Supervision in Southern Hilly Region, Ministry of Natural Resources, Changsha 430103, China

⁴ Department of Remote Sensing and GIS, Faculty of Geography, University of Tehran, Tehran 14178-53933, Iran; ali.darvishi@ut.ac.ir (A.D.B.); masoud.soleimani@ut.ac.ir (M.S.)

* Correspondence: yzqin60010@ecut.edu.cn (Y.Q.); cl@img.net (L.C.)

Abstract: It is important to analyze the trend in land use changes and assess the suitability of resource development for protecting natural resources, developing ecological industries, and land use planning issues. Ruijin City is located in South Jiangxi and has abundant resources for red tourism development. By analyzing the landscape changes in land use and the spatial distribution characteristics of local red culture resources, a supervised machine learning-based prediction model was constructed to quantitatively assess the suitability of red tourism development in a geographic information system (GIS) and the R language environment using geographical, economical, and human-related datasets. The results revealed that: (i) the increasing of human activities and economic vitality provide a beneficial social environment for the development of tourism resources; (ii) highly concentrated red resources, or those with special significance, are conducive to developing red tourism resources; (iii) preferentially, central–eastern Ruijin was followed by the extension areas to peripheral towns, which are potentially suitable areas for the development of red scenic spots. Generally, the findings of this study were consistent with the conventional cognitions and lessons on tourism development, and the constructed evaluation system is expected to be promoted to similar research.

Keywords: suitability assessment; machine learning; landscape changes; red tourism; Ruijin City



Citation: Qin, Y.; Cao, L.; Li, W.; Darvishi Bolorani, A.; Li, Y.; Ke, X.; Soleimani, M.; Yu, Q.; Zhou, C. Suitability Assessment Method of Red Tourism Development Using Geospatial and Social Humanity Data: A Case Study of Ruijin City, East China. *Sustainability* **2023**, *15*, 8582. <https://doi.org/10.3390/su15118582>

Academic Editors: Colin Michael Hall, Nicholas Wise and Takamitsu Jimura

Received: 15 April 2023

Revised: 15 May 2023

Accepted: 23 May 2023

Published: 25 May 2023



Copyright: © 2023 by the authors. Licensee MDPI, Basel, Switzerland. This article is an open access article distributed under the terms and conditions of the Creative Commons Attribution (CC BY) license (<https://creativecommons.org/licenses/by/4.0/>).

1. Introduction

Tourism resource development plays a key and positive role in urbanization, and it can not only promote the economic development of existing cities but also accelerate the expansion and construction of cities. To obtain a clear vision of future tourism development, it is essential to understand the land use pattern changes in tourist development areas based on the characteristics and connotations of the local culture [1–4]. Red tourism, which is a special kind of tourism industry that integrates tourism visits, cultural features study, and political education with Chinese characteristics, represents the traditional culture of the Chinese nation and the revolutionary spirit of the Chinese people, which brings the multiple benefits of culture, economy, and society [5,6], especially for maintaining a national communist identity and developing a socialist country with Chinese characteristics in a rapidly changing China [7]. The red culture, which is consistent with the spirit of the Chinese nation, includes striving for self-improvement, unity of knowledge and action,

being people oriented, pursuing truth, and being willing to dedicate oneself, and it is the continuation of traditional Chinese culture. Consequently, it is a critical prerequisite to assess the suitability of red tourism development to the prosperity of the ecotourism industry [8,9].

The land use pattern indicates the spatial–temporal characteristics of human and economic activities that directly impact the landscape and ecosystem functionality [10–12]. Conversely, the development of human activities and social structure will actively promote the changes in land use and ecological services [13–16]. In order to analyze the development trend in human activities and socio-economic conditions, the land use pattern (LUP) in consecutive years should be identified [17–19]. Various development indices about landscape changes are usually used for analyzing the spatial–temporal characteristics of landscape ecological effects on urban development [20,21]. The interaction of urbanization and ecosystem services are explored in the literature. For instance, Ou-Yang et al. [20,21] used hot spot and spatial autocorrelation analysis to discover the long-term correlation between urbanization and ecosystem services in several urban agglomeration areas [20]. Alphan et al. (2022) [22] determined the relationships of residential development with the spatial–temporal dynamics of land use in southern coast of Turkey by analyzing multi-level pattern metrics [22]. Duan et al. [23] predicted the trend in land use/cover by analyzing the evolution of landscape pattern in Sanjiangyuan region of the Qinghai–Tibet Plateau. They concluded that the dramatic changes in land use/cover will impact ecosystem services, especially in the ecologically fragile areas.

Tourism development is closely related to many disciplines such as geography, culture, policy, business, and economy. The tourism suitability assessment is usually carried out by qualitatively analyzing the spatial distribution of tourism resources and developing (semi-)quantitative environmental indices [24–26]. For example, Fadafan et al. [27] used four categories of evaluation factors including environment, economy, socio-culture, and managerial to assess the suitability of the area for intensive tourism development. We need to mention that the evaluation factors have relatively different importance in tourism suitability assessment methods [28]. Accordingly, different methods such as information value (IV) [29], weight of evidence (WofE) [30], and analytic hierarchy process (AHP) [31] have been introduced in geographical information system (GIS) by integrating various indices to suitability assessment of tourism development [15,32–35].

Various machine learning algorithms, especially support vector machine (SVM) [36], random forests (RF) [37], extreme gradient boosting (XGB) [38], logistic regression (LR) [39], and convolutional neural network (CNN) [40], are widely used in many research fields of geoscience. Remote sensing (RS) image classification is a common tool for land use survey, which has become more robust with the introduction of machine learning algorithms [41–46]. Supervised machine learning algorithms have obtained promising results in mineral prospectivity mapping [47–50], geo-hazard mapping and geo-risk assessment [51–54], biomass estimation [55–58], and dust source susceptibility mapping [59,60].

In this paper, to promote sustainable tourism development in Ruijin City, the Landsat 8-OLI images are used for land use classification and landscape pattern analysis. The RF-based regression model is constructed by integrating multiple data from natural geography, human economy, and ecological environment to quantitatively assess the suitability of red tourism resources development and then provide recommendations for further land use planning and ecological protection.

2. Materials and Methods

2.1. Study Area

Ruijin City, located in the climate transition zone of Central and southern China (Figure 1), is characterized by humid climate, abundant rainfall, sufficient sunshine, and four distinctive seasons. The southeast of Ruijin is rolling vein of the Mount Wuyi, and the northwest is surrounded by mountains. There is a notable variety of landforms in Ruijin, and denuded hills, eroded mountains, karst areas, and river valley accumulation terraces

are widely distributed. In total, 17 townships in Ruijin jurisdiction are the main residences of the Hakka people and the important birthplaces of the Hakka culture. Well known as one of the important birthplaces of the Hakka culture and the “cradle of the People’s Republic”, Ruijin is the famous “Red Capital”, with numerous revolutionary sites and profound red culture.

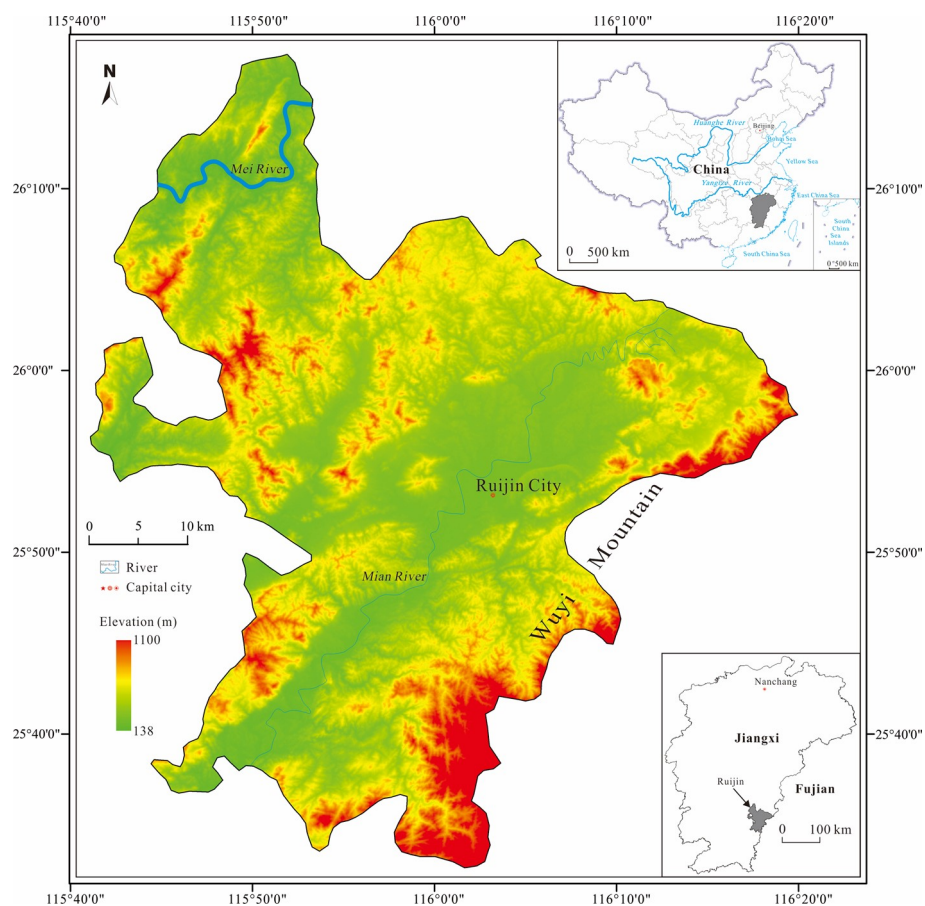


Figure 1. The study area in Jiangxi Province, China.

2.2. Dataset

As shown in Table 1, in this study, three datasets including remote-sensing-based land use change maps (2013 to 2021), spatial distribution of local red culture resources (RCRs), and tourism development index based on environmental factors such as geography, culture, policy, business, and economy were used.

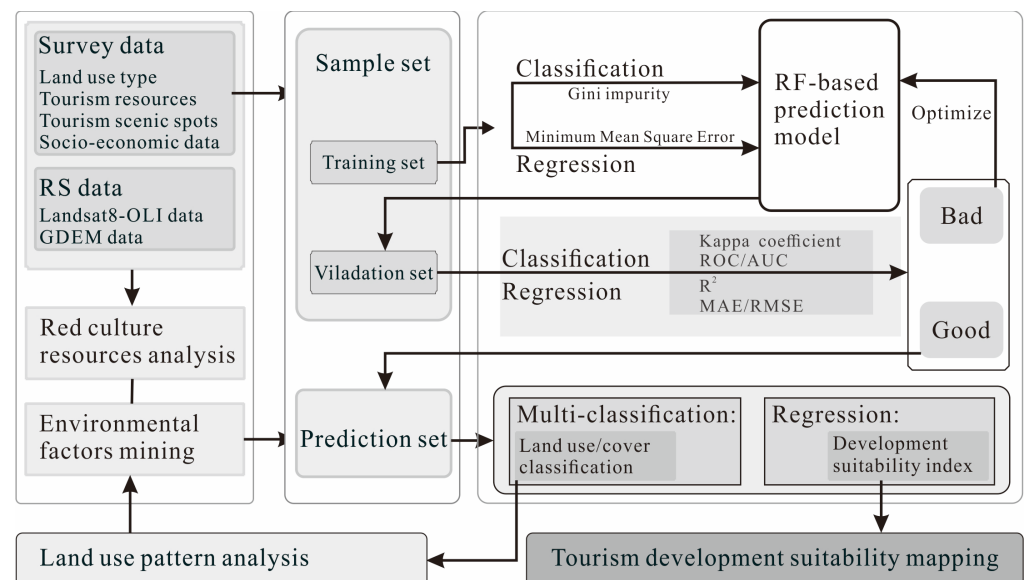
The study area was about 2432 km² and was divided into a total of about 2.7 million grids with the mesh size of 30 m × 30 m, according to resolution of Landsat image and survey density of multi-source data, which could meet the accuracy requirements of LUP analysis and tourism development assessment.

Table 1. Specifications of parameters used for suitability assessment of tourism development.

Data Type	Source	Purpose
Remote sensing data	Landsat 8 OLI images of 2013, 2017, and 2021 DEM of 30 m resolution from GDEM V3	land use classification, landscape pattern analysis
Development data of scenic spot	Total annual income Total annual tourist numbers Scenic spot score Revolutionary sites Cultural relics Population density	Dependent variable of sample for evaluation model
Environmental factors	Land price Slope Elevation Roads Hotel classes	Independent variable of dataset for evaluation model

2.3. Methodology

On the basis of the field survey and RS data acquisition, image pre-processing, information extraction, and land use classification were carried out using ENVI 5.3 (The Environment for Visualizing Images, <https://envi.geoscene.cn/>) and its QGIS plugin EnMAP-Box [61]. The trend in LUP was analyzed by calculating landscape pattern index in Fragstats 4.2 [62,63]. Various environmental factors were explored and integrated. The distribution characteristics of RCRs were described in ArcGIS 10.2 (<https://support.esri.com/>). Finally, the RF-based regression model was constructed for suitability assessment of tourism development in R programming environment. The research methodology is schematically illustrated in Figure 2.

**Figure 2.** Methodology for tourism development suitability assessment.

2.3.1. RF Classification and Regression

The RF is a supervised ensemble learning algorithm, based on decision tree [64], constructing a series of weak learner (tree) by training sample data. The learners were integrated to generate an optimized model. It predicted by adopting a method similar to “democratic voting”, meaning that the minority was subordinate to the majority when in the face of classification problems. It took the arithmetical average of weak learners as the final prediction result while it dealt with continuous problem [65].

There are two random processes in RF: one is Bagging and the other is random subspace of feature variables. The Bagging (namely bootstrap aggregating) is the base algorithm for RF construction [65], which builds a new sample set by randomly sampling with replacement from the original data. The process that randomly chooses several of the variables from all the features to generate every decision tree is conducive to solving the problems of under-or over-fitting.

Gini impurity (Gini index) is the basis of node splitting for the binary classification tree. It measures the probability that a randomly selected sub-item from a dataset is incorrectly divided into other class. To a feature A in node n , which has K classes, the occurrence probability of class k is p_k , and the Gini index of A ($Gini(A_n)$) is defined as:

$$Gini(A_n) = \sum_{k=1}^K p_k(1 - p_k) = 1 - \sum_{k=1}^K p_k^2 \quad (1)$$

Suppose D is sample number of feature A in node n , and it is divided into two parts, left and right. The Gini impurity of parent node (to n) $Gini(D, A_n)$ is expressed as:

$$Gini(D, A_n) = \frac{D_L}{D} Gini(A_L) + \frac{D_R}{D} Gini(A_R) \quad (2)$$

where the D_L and D_R , respectively, are the sample number of left and right part, and $Gini(A_L)$ and $Gini(A_R)$ are the left and right Gini index in node n . To the construction of RF, the node n with the smallest Gini is the optimal splitting point for a certain feature A in the process of regression tree.

Minimum Mean Square Error (MMSE) is used as splitting principle in constructing binary RF regression model. At the splitting node n , D is the sample number of its parent node for feature A , being divided into right and left parts. The expression of the MMSE in this node is written as:

$$MMSE(D, A_n) = \min \left(\min_{y_i \in A_L} \sum (y_i - \bar{y}_L)^2 + \min_{y_i \in A_R} \sum (y_i - \bar{y}_R)^2 \right) \quad (3)$$

where A_L and A_R are the feature values of left and right parts at the node n ; y_i is the value of feature; and \bar{y}_L and \bar{y}_R are the mean value of feature A_L and A_R . The node, which has the MMSE in A_L and A_R and the smallest sum of the MSE for feature A , is the optimal splitting node.

2.3.2. Model Construction

The step-wise procedure for RF construction is as follows:

- (i) Divide samples into training and validation sets according to the ratio of 7:3, and a new training set will be generated by using the Bagging method;
- (ii) Randomly select m features from M . Usually, m is equal to \sqrt{M} . Construct a decision tree by using Gini index or MMSE method;
- (iii) Create a series of trees to construct RF model;
- (iv) Use the RF model to classification and regression if it acquires the required performance in validation step, or it will be revised and optimized.

2.3.3. Performance Evaluation

The performance of classification model is evaluated using confusion matrix [66]. The true positive rate (TPR), true negatives rate (TNR), and overall accuracy (OA) can indicate the model performance to a certain extent. The Kappa coefficient (KC) and receiver operating characteristic (ROC) curve would be more appropriate when the samples are in a smaller size or unbalanced structure. The higher KC and AUC (namely area under the ROC curve) that are all close to 1 mean the better performance of a classifier [48].

To evaluate the performance of regression models, several metrics such as R-square (R^2), mean absolute error (MAE), and root mean square error (RMSE) can be used. R^2 reflects the overall matching of the prediction and observation results. MAE is the mean of absolute error, which can well describe the actual prediction error. RMSE directly compares the deviation of prediction and observation: the lower value shows the better the prediction accuracy. These metrics are calculated using the Equations (4)–(6):

$$R^2 = 1 - \frac{\sum (y_i - \hat{y}_i)^2}{\sum (y_i - \bar{y}_i)^2} \quad (4)$$

$$MAE = \frac{1}{N} \sum_{i=1}^N |y_i - \hat{y}_i| \quad (5)$$

$$RMSE = \sqrt{\frac{1}{N} \sum_{i=1}^N (y_i - \hat{y}_i)^2} \quad (6)$$

where, N is the total number of samples, y_i is observed value, \hat{y}_i is predicted value, and \bar{y}_i is average value of samples.

2.3.4. Landscape Pattern Index

The landscape was composed of relatively homogeneous ecological elements on the ground, which generally were divided into patch, corridor, and matrix. Landscape pattern index referred to two aspects, namely, landscape pattern and landscape index. Landscape pattern expressed the spatial structure characteristics of the landscape, including the type, number, and spatial distribution form of landscape components. The landscape index was a simple quantitative indicator, usually reflecting the composition and characteristics of the landscape structure [67,68].

With the help of ArcGIS and Fragstats, the structural and functional pattern index could be calculated based on the classification images. The patch-based indexes indicated the characteristics of a single patch, the class-based indexes reflected the characteristics of the same patches, and the landscape-based indexes showed the overall structural characteristics of different patches combination. In this study, five pattern indices, proportion of patches in landscape (PLAND), largest patch index (LPI), fractal dimension (FRAC), Shannon diversity index (SHDI), and dynamic degree (DE) were calculated to analyze the distribution characteristics and spatial change in land use types. More details on the derivation of the formulae for calculating these indexes were given in Mcgarigal [62].

3. Results and Discussion

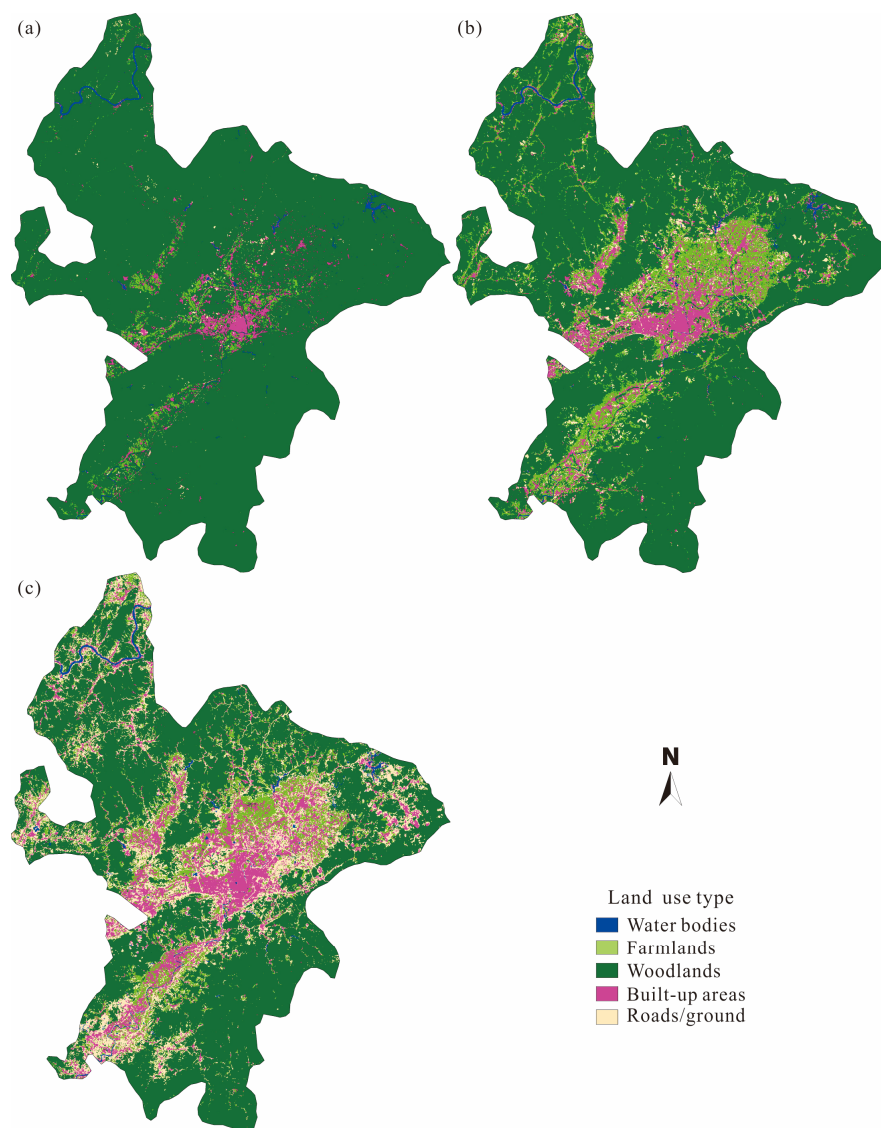
3.1. Land Use Change Analysis

The Landsat 8-OLI images of April 2013, April 2017, and March 2021 were used for land use classification based on the China National Standard of Current land use classification (GB/T 21010-2017). According to the local knowledge about land use in Ruijin and the separability of sample classes, five land use types, including water bodies, farmlands, woodlands, built-up areas, and roads/ground, were classified by using the RF classifier. The samples for constructing and testing classifier were obtained from Gaofen satellite images, Google Earth high resolution imagery (2013 and 2017), and a field survey (2021). Nine spectral indices, including soil-adjusted atmospherically-resistant vegetation index (SARVI) [69], normalized difference water index (NDWI) [70], normalized difference build-up soil index (NDBSI) [71], brightness–greenness–wetness from Tasseled Cap Transform (TCT) [72], and hue–saturation–value from HSV transformation [53] were used as classifier feature variables. Table 2 shows the parameters of the RF classifier and corresponding validation metrics for three investigation years (2013, 2017, and 2021).

Table 2. Parameters of the RF based classification models.

Parameters		Year		
		2013	2017	2021
RF classifier construction	No. of trees	95	105	100
	No. of feature variables	3	3	3
RF classifier performance	Overall accuracy	96.25	96.58	97.99
	Kappa coefficient	87.86	88.23	90.21

Visual interpretation of the land use maps (Figure 3) revealed that (i) although the woodlands showed a decreasing trend, it was still the dominant land use type in the study area; (ii) the built-up areas were mainly concentrated in central Ruijin in 2013 and then gradually expanded and dispersed to nearby areas along the urban roads, showing that the municipal construction of Ruijin was continuously expanding with rapidly economic growth; (iii) the farmlands and roads/ground intricately expanded from 2013 to 2021, and it was anomalous that the expansion of roads/ground was faster than farmlands (Figure 3b,c).

**Figure 3.** Land use maps ((a), 2013; (b), 2017; (c), 2021) obtained from Landsat 8-OLI imagery and RF classifier.

3.2. Landscape Pattern Analysis

The following pattern indices were analyzed to show the spatial changes in landscape patterns. Where LPI and PAFRAC represented the characteristics of individual units, LPI and CONTAG expressed the spatial configurations of landscape components, and DE showed the overall diversity of the landscape.

The consistent trend in PLAND and LPI (Figure 4a,b) showed (i) the coverage rate of woodlands dropped from 94.15% in 2013 to 61.31% in 2021; (ii) the proportion of built-up areas and roads/ground increased from 2013 to 2021, but the farmland increased first and then sharply decreased, which may have been due to the misclassification farmlands in following in March 2021; (iii) these two indices were scarcely changed for water bodies. The mean FRAC (Figure 4c) of the inherited land use types such as water bodies and woodlands showed a steady downward trend. Nevertheless, the farmlands, built-up areas, and roads/ground that were related to human activities changed sharply. For the DE (Figure 4d), woodlands increased with a range of 4.98%, and other land use types increased as well; the 4-year periods' growth of water was 4.91%; the change range of roads/ground should have been far less than 450.10%, and, of the farmlands, it should have been more than 45.01%; it was acceptable that the built-up areas increased by 45.96%.

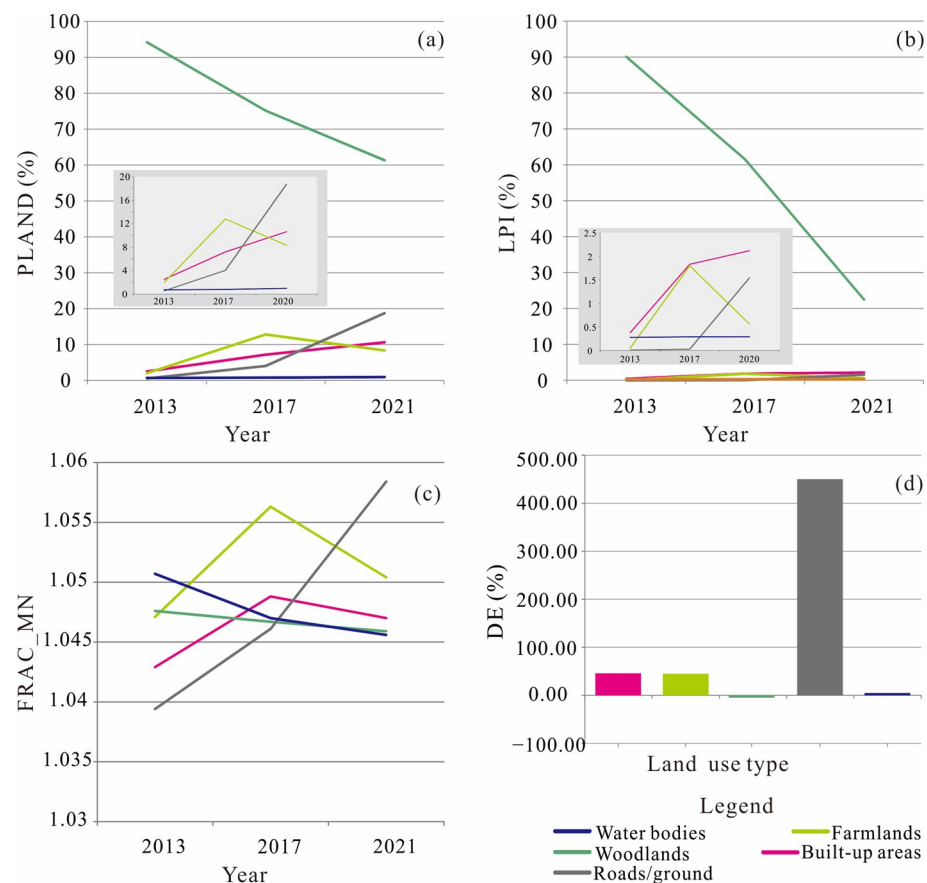


Figure 4. Land use-based landscape pattern analysis using (a) PLAND; (b) LPI; (c) FRAC_MN; (d) DE indices for different investigation years.

It could be argued that the continuous diffusion of built-up areas, farmlands, and roads/ground squeezed and dispersed the forest lands. The built-up areas and roads/ground were gradually concentrated in large areas, and, on the contrary, the water bodies dispersed.

The trend in landscape changes based on the landscape indices from 2013 to 2021 is shown in Figure 5. Hence, LPI decreased from 90.03% to 22.47% and CONTAG decreased from 87.27% to 52.43%, which indicated that the dominant land use types significantly reduced. Meanwhile, the fragmentation degree of all land use types increased. The

downward trend in SHDI and FRAC_MN showed that the fragmentation degree of all land use types was getting higher with the increment of human activities. Landscape pattern analysis in both land use and landscape levels revealed that the land use became more abundant, and the landscape spatial pattern became more complex.

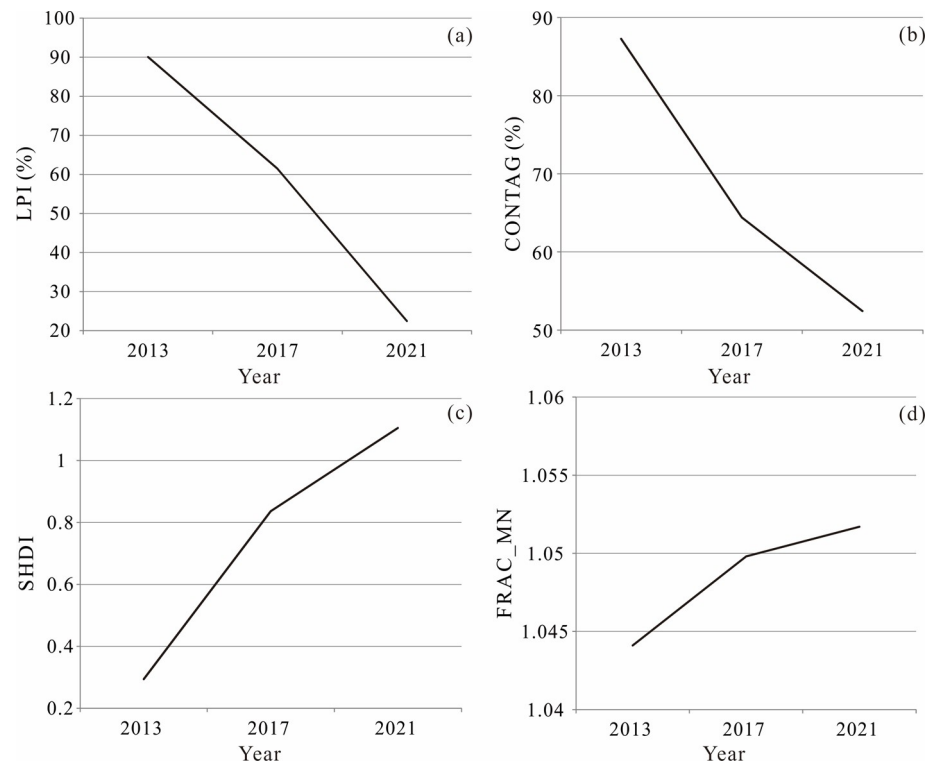


Figure 5. Landscape pattern analysis using (a) LPI; (b) CONTAG; (c) SHDI; (d) FRAC_MN indices for different investigation years.

These analysis results in Sections 3.1 and 3.2 indicate that the land use types with their landscape pattern are undergoing significant changes under human activities, and these changes usually promote economic growth and are beneficial for tourism development.

3.3. Analysis of Red Culture Resources

3.3.1. Spatial Distribution of the RCRs

As the famous “Red Capital”, Ruijin has more than 180 former sites of revolutionary [73]. A total of 125 revolutionary sites have been acquired from points of interest (POI) and other public data on the internet by coordinate picking. Most of the RCRs (~77.6%) are centrally distributed in six townships in central Ruijin (Figure 6a). There are 24 sites in Yeping, 23 in Huangbai, 17 in Jiubao, 13 in Shazhouba, 11 in Rentian, and 9 in Yunshishan. Xianghu, which is the seat of the government of Ruijin, has 6 sites, while the other 10 townships have 22 sites.

To intuitively visualize the spatial aggregation of the RCRs, the kernel density distribution was generated with a grid resolution of 30 m and a radius of 5 km (Figure 6b). It showed that the RCRs were distributed in two different zones: one was the strip zoning of Jiubao–Yunshishan, and the other was an annular belt consisting of Rentian–Yeping–Xianghu–Shazhouba–Huangbai. In addition, a few sites were clustered in Dabaidi and Ridong, while other individual sites were scattered in peripheral towns.

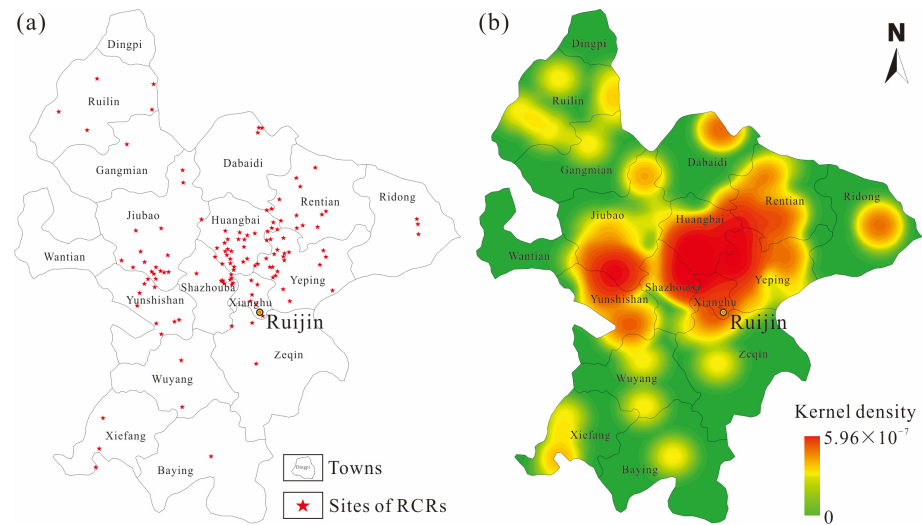


Figure 6. Distribution (a) and kernel density (b) of RCRs in Ruijin.

3.3.2. Relationship of RCRs and Red Tourism Scenic-Spot (RTS)

The construction scale of RTS is highly positively correlated with the spatial density of RCRs. For example, the Yeping tourism areas, which is one of the most well-preserved red tourism scenic areas in China, includes multiple scenic spots, such as the former sites of the 1st Soviet Congress and Central Bureau of the Communist Party of China (CPC) Soviet Region, Bosheng Fortress, Gonglue Pavilion, and the Red Army Martyrs Monument, covering an area of more than 106,600 m². The RTSs mentioned in this study are built on the basis of the RCRs. They indicate that the high concentration of RCRs is conducive to spatial expansion and cost reduction in the scenic spot construction.

The zonal aggregation of RCRs is in favor of construction of red scenic areas, for instance, the Cradle Scenic group of the Republic, including Yeping, Hongjing, and the Chinese Soviet Memorial Garden, is located in the annular belt mentioned above. The occurrence of this tourism construction mode greatly improves the development quality of tourism scenic spots and their downstream industries. The red scenic spots, which are built on single red resource, such as the Former Residence of Mao Zedong in Wuyang and the Martyrs Cemetery of Mao Zeqin in Zeqin, also have special educational significance and positive social benefits. The townships lacking revolutionary sites or cultural relics, such as Wantian and Dingpi, are still possible to explore local distinctive cultures related to red resources for developing tourism scenic spots and ecological tourism industries.

3.4. Suitability Assessment of Red Tourism Development

3.4.1. Assessment Factors

The analysis based on LUP and RCRs shows that Ruijin has the required conditions to develop red tourism resources. To a certain extent, the planning and construction of red scenic spots depends on the spatial distribution of RCRs. Accordingly, nine factors, including the slope, altitude, land use, population density, land price, distance to road, distance to hotel, distance to cultural–relic/historic sites, and distance to revolutionary sites, were acquired from Internet POI and a recent Statistical Yearbook as the assessment factors (feature variables). The data of the factors about the socio-economy and humanity are the annual averages of year 2021, published by the government.

According to the influence of these factors, buffer zones for the distance to revolutionary sites, distance to cultural–relic/historic sites, distance to hotel, and distance to road were analyzed (see Figure 7). For the distances from infrastructures to roads and hotels, a maximum buffer radius of 1000 m was generated, with an interval of 200 m. The distances from the key evaluation targets to revolutionary sites and cultural–relic/historic sites were

buffered within 2500 m, with a 500-m interval. The spaces that exceeded the maximum buffer radius were set to an extra-large value, for example, 999,999.

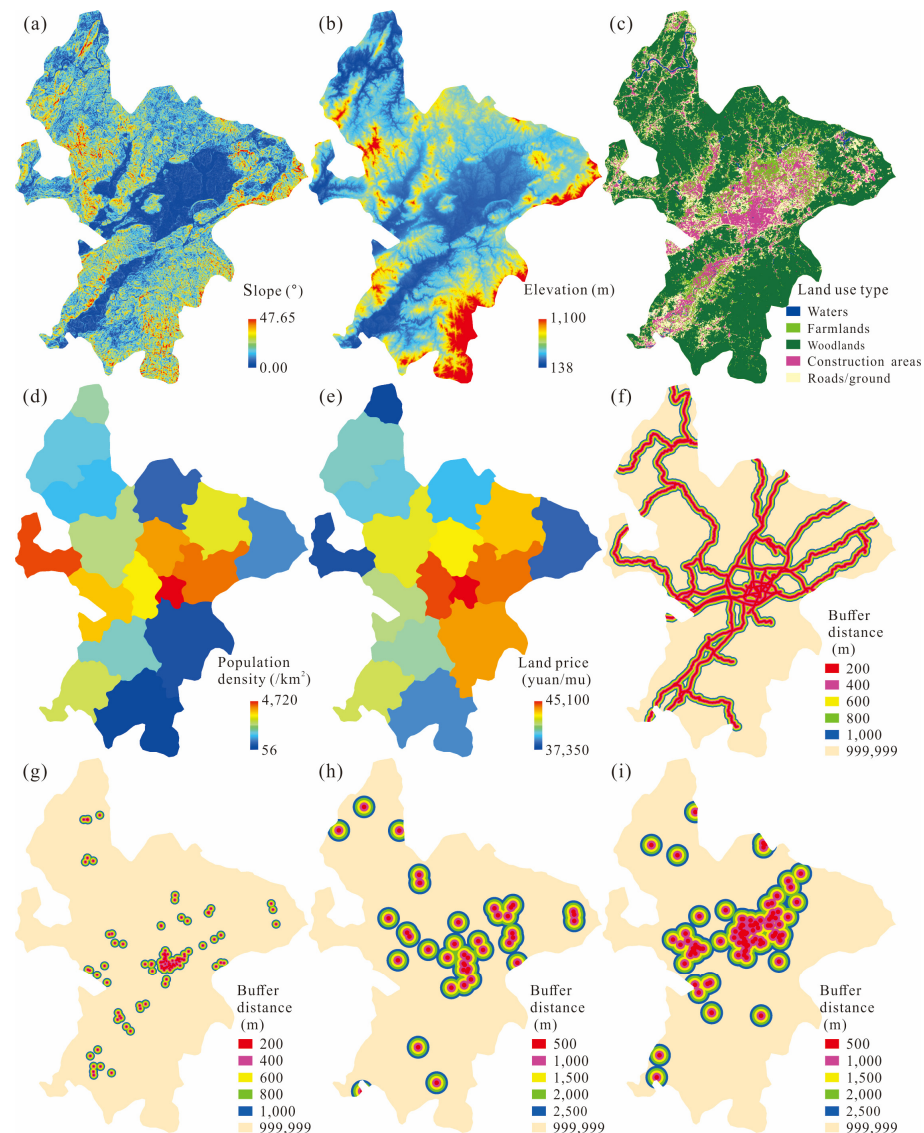


Figure 7. Feature variables ((a) slope; (b) altitude; (c) land use; (d) population density; (e) land price; (f) distance to road; (g) distance to hotel; (h) distance to cultural-relic/historic sites; and (i) distance to revolutionary sites).

3.4.2. Response Variables

Qin et al. [48] argued the critical role of response variables in supervised prediction models. Ten typical scenic spots samples, which covered an area of about 14 km², were selected for suitability assessment from existing red tourism scenic areas (Figure 8 and Table 3). A new index, named development suitability index (DSI), which measured the development scale and income level of the tourism scenic spot, was developed (Equation (7)) as response variable (target label) of the samples for constructing the regression model. The estimated DSI by regression represented the degree of development suitability of red tourism resources.

$$DSI = w_1 \times R_{norm} + w_2 \times N_{norm} + w_3 \times S_{norm} \quad (7)$$

where R_{norm} , N_{norm} , and S_{norm} are the normalized values of the indexes of the annual overall revenues R , annual tourist number N , and scenic spot score S , respectively, for

each sample scenic spot, and w_1 , w_2 , and w_3 are the corresponding weights of these three factors. Here, according to the conventional understanding to scenic spot development, the weights of R , N , and S were set to 0.5, 0.3, and 0.2, respectively. R and N are the proportion of the annual tourism revenues and tourist number for every sample scenic spot in total of Ruijin City, and S is their respective grade ratio, namely, the proportion of rating level in the highest.

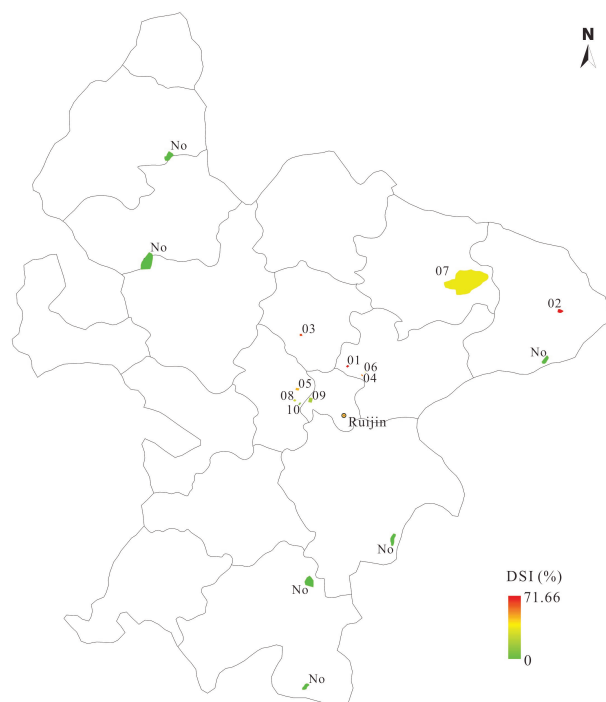


Figure 8. Development suitability index (DSI) of the sample scenic spots of red tourism.

Table 3. Development suitability index (DSI) of sample scenic spot in Ruijin.

Code	Scenic Spot	Area Covered (ha)	DSI (100%)
01	Polar Ocean Park	5.53	71.66
02	Wooden Fish Mountain	19.95	71.46
03	Hongjing	6.21	67.94
04	Cradle of the Republic	2.80	67.72
05	2nd Soviet Congress of the Soviet Republic of China	9.74	60.45
06	Yeping	0.67	53.98
07	Arhat Rock	869.39	44.18
08	Happy Flower Sea of Red Capital	5.80	40.41
09	Historical Museum of Central Base	19.95	33.53
10	Former Site of the Central Revolutionary Military Commission	4.40	10.92
No	Non-Scenic Space	456.92	0

Table 3 shows the DSI of the selected ten typical scenic spots and several non-scenic sites. Non-scenic sites covered the areas where the forest was dense and inaccessible, traffic was inconvenient, or the land was protected as the main farmland. These were improper or not allowed for tourism development. The DSIs of the non-scenic sites were set to zero (i.e., the minimum for regression). In addition, the areas of the sample spots were roughly determined according to their approximate outline. The DSI was calculated using the average of annual overall revenues, annual tourist number, and scenic spot score/grade in 2020 and 2021 for all the samples.

3.4.3. Construction and Evaluation of Regression Model

The samples were randomly divided into training and validation sets at a ratio of 7:3. The RF regression algorithm was used to construct a suitability assessment model, containing 600 decision trees by using a training set. The mean of the squared residuals and the goodness-of-fit (namely var explained in R) of the constructed model were 0.13 and 99.97%, respectively, which meant an excellent regression performance. With applying the constructed model to the validation set, R^2 , MAE, MSE, and RMSE were 99.98%, 0.14, 0.10, and 0.32, respectively. These statistics indicated that the constructed regression model had reliable performance.

The importance ranking of feature variables indicated the contribution of assessment factors to the constructed model. A higher importance ranking of a feature variable indicated a higher correlation between it and the response variable. As shown in Figure 9, the results of the performed importance ranking using %IncMSE and IncNodePurity were similar to each other. Our result revealed that the land price was the most important factor for suitability assessment of tourism development since it was closely related to the geographical environment, land use types, and human activities. Population density, revolutionary sites, altitude, and cultural-relic/historic sites were the less important factors. However, these factors indicated that human activities, geographical conditions, and red cultural resources were related to the development of red tourism. On the other hand, road/traffic, hotels, and slope were not closely related to tourism development. For the land use types, a combination of multiple classes was important to tourism development. It is worth mentioning that these findings were consistent with the conventional cognition of tourism development in Ruijin.

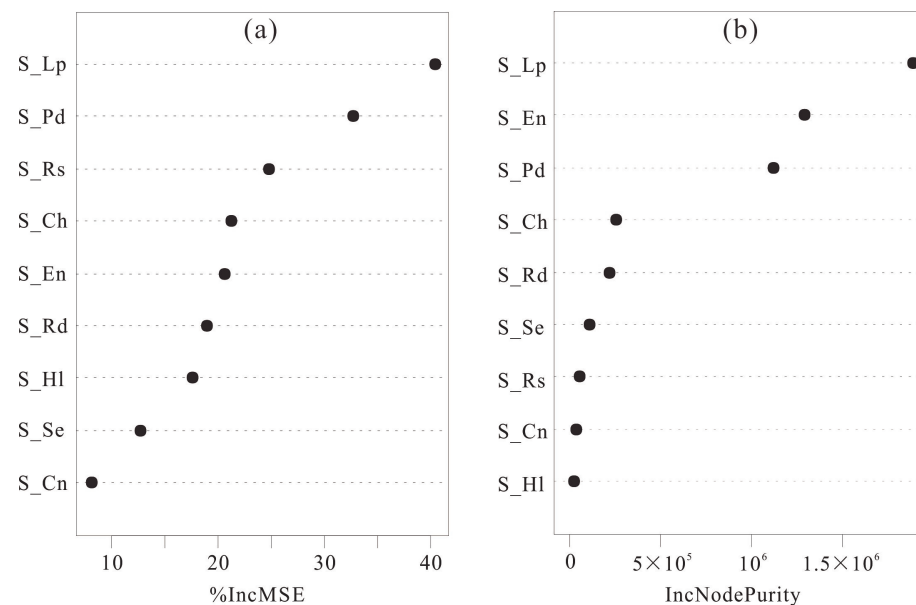


Figure 9. Importance ranking of feature variables ((a) %IncMSE; (b) IncNodePurity).

3.4.4. Red Tourism Suitability Mapping

The development suitability index (DSI) of red tourism resources was predicted by applying the RF-based regression model (Figure 10a). The DSI map was graded into extremely high, high, medium, low, and extremely low areas by using Jenks natural breaks [74] clustering method (Table 4, Figure 10b).

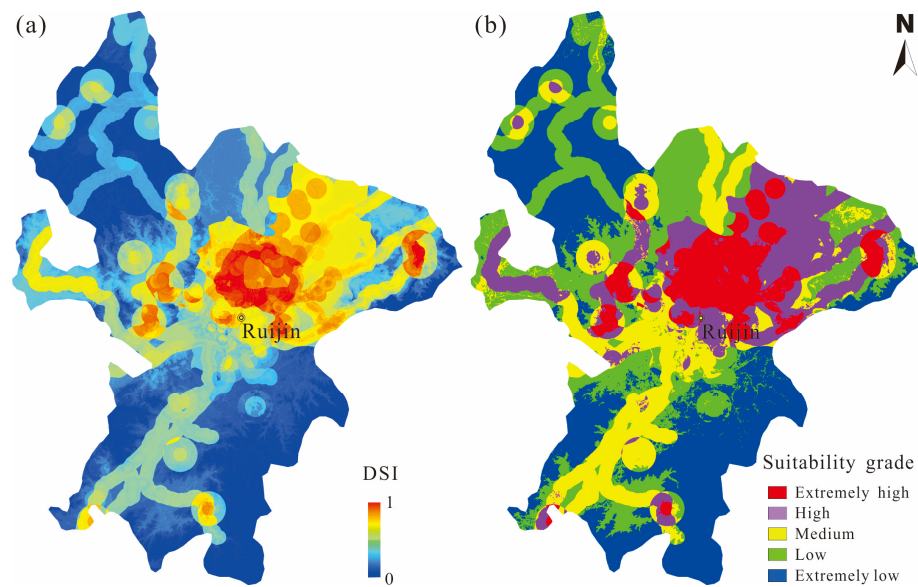


Figure 10. Result of the RF-based regression model for suitability assessment, showing the suitability index map (a) and its zoning (b) for tourism resources development.

Table 4. Five grades of development suitability index (DSI) zoning for red tourism resources in Ruijin.

Grade	Interval of DSI (%)	Area Covered (km ²)	Percentage of Land Occupied (%)
Extremely high	0.72–1.00	254.25	10.45
High	0.52–0.72	388.92	15.99
Medium	0.32–0.52	431.70	17.75
Low	0.13–0.32	624.73	25.68
Extremely low	0.00–0.13	733.17	30.14

The results revealed that the extremely high suitability areas that covered 10.45% of the study area were mainly distributed in central Ruijin, where the terrain was flat, mostly, on the west, and northeast of the downtown area, excluding Xianghu. They showed that the highly clustered red resources were more conducive to the planning and construction of red tourism scenic spots. High land price and the large population density were not beneficial to tourism development. The high suitability areas covered 15.99% of Ruijin and were mainly located on the east and west sides of the extremely high suitable areas, while others were located in the township centers of north and south Ruijin. This indicated the possibility of developing tourism relying on individual red resources. The medium suitability areas were basically distributed along main roads of towns, indicating that the planning and development of red tourism could still be carried out in a favorable geographical and economic environment. The low and extremely low suitability areas covered 55.82% of Ruijin, which were mainly distributed in the northwest and south of the study area. These areas were heavily covered by forest in mountainous areas without convenient transportation systems.

4. Conclusions

Using remote-sensing-based land use pattern analysis and practical red culture resources, in combination with geospatial environmental factors such as humanity, economy, and geography in a random forest-based model, a suitability assessment procedure was implemented for red tourism resources development in Ruijin City, South China. According to our results, it can be concluded that:

- (i) Increasing the scope and intensity of human activities with continuously improved economic vitality provides a benign social environment for developing tourism resources.
- (ii) Highly concentrated red culture resources are conducive to the large-scale development of red tourism scenic spots. This can be developed relying on a single red resource or by exploring local characteristic culture related to red resources.
- (iii) Environmental factors such as altitude, land price, population density, revolutionary sites, and cultural–relic/historic sites contribute significantly to the construction of the suitability assessment model, meaning that their feature variables are more closely related to the development of red tourism resources.
- (iv) The further development potential areas of red tourism resources are preferentially located in the central and eastern Ruijin, including the northeast and west of the downtown area, followed by the areas distributed around the high potential sites or along the main roads.
- (v) The importance ranking of the environmental factors and assessment results based on developed suitability model are consistent with the local knowledge on red tourism in Ruijin.
- (vi) From a local perspective, in the last eight years, the landscape pattern of Ruijin has experienced significant changes, showing that the intensity and influence of human activities is gradually increasing, and the economic vitality is constantly improving.

In addition, the supervised machine learning used in this study RF classification and regression performed excellently on development suitability evaluation. The generated suitability zoning map was generally consistent with the qualitative understanding to tourism development. This meant that this study is also expected to constitute a methodological system suitable for such research in urbanization processes.

Author Contributions: Conceptualization, Y.Q.; methodology, Y.Q. and L.C.; software, Y.Q., L.C., Q.Y. and Y.L.; writing—original draft preparation, Y.Q., L.C. and W.L.; writing—review and editing, Y.Q., M.S. and A.D.B.; visualization, X.K. and C.Z.; supervision, Y.Q. and L.C.; project administration, Y.Q.; funding acquisition, Y.Q. All authors have read and agreed to the published version of the manuscript.

Funding: This research was funded by the Science and Technology Research Project of Jiangxi Provincial Department of Education (Grant No. GJJ210709), also supported by the Fund of Key Laboratory of Natural Resources Monitoring and Supervision in Southern Hilly Region, Ministry of Natural Resources (Grant No. NRMSSHR-2022-Z05) and the Fund of National Key Laboratory of Science and Technology on Remote Sensing Information and imagery Analysis, Beijing Research Institute of Uranium Geology (Grant No. 6142A010411).

Institutional Review Board Statement: Not applicable.

Informed Consent Statement: Not applicable.

Data Availability Statement: Applicable data are contained within this article.

Conflicts of Interest: The authors declare no conflict of interest.

References

- Ning, C.; Hoon, O.D. Sustainable development strategy of tourism resources offered by regional advantage: Exploring the feasibility of developing an ‘exotic culture’ resource for Weihai City of China. *Procedia Eng.* **2011**, *21*, 543–552. [[CrossRef](#)] [[PubMed](#)]
- Jin, Y.; Xi, H.; Wang, X.; Ren, X.; Yuan, L. Evaluation of the Integration Policy in China: Does the Integration of Culture and Tourism Promote Tourism Development? *Ann. Tour. Res.* **2022**, *97*, 103491. [[CrossRef](#)]
- Xiao, Y.; Tang, X.; Wang, J.; Huang, H.; Liu, L. Assessment of coordinated development between tourism development and resource environment carrying capacity: A case study of Yangtze River economic Belt in China. *Ecol. Indic.* **2022**, *141*, 109125. [[CrossRef](#)]
- Wang, Q.; Yang, L.; Yue, Z. Research on development of digital finance in improving efficiency of tourism resource allocation. *Resour. Environ. Sustain.* **2022**, *8*, 100054. [[CrossRef](#)]

5. Zhao, S.; Timothy, D.J. Governance of red tourism in China: Perspectives on power and guanxi. *Tour. Manag.* **2015**, *46*, 489–500. [[CrossRef](#)]
6. Zuo, B.; Gursoy, D.; Wall, G. Residents' support for red tourism in China: The moderating effect of central government. *Ann. Tour. Res.* **2017**, *64*, 51–63. [[CrossRef](#)]
7. Li, Y.P.; Hu, Z.Y.; Zhang, C.Z. Red tourism: Sustaining communist identity in a rapidly changing China. *J. Tour. Cult. Chang.* **2010**, *8*, 101–119. [[CrossRef](#)]
8. Yin, X.Y.; Zhu, H.; Gan, M.Y. Study on product characteristics and developing modes of red tourism. *Hum. Geogr.* **2005**, *2*, 34–37 + 76. (In Chinese with English Abstract)
9. Chai, J.X. The Integrated Development of Red Tourism and Marine Characteristic Town under the Background of One Belt, One Road. *J. Coast. Res.* **2020**, *112*, 77–80. [[CrossRef](#)]
10. Li, X.B. Explanation of land use changes. *Prog. Geogr.* **2002**, *3*, 195–203, (In Chinese with English Abstract).
11. Peng, J.; Wang, Y.L.; Zhang, Y.; Ye, M.T.; Wu, J.S. Research on the influence of land use classification on landscape metrics. *Acta Geogr. Sin.* **2006**, *2*, 157–168. (In Chinese with English Abstract)
12. Wang, Y.; Li, X.; Xin, L.; Tan, M. Farmland marginalization and its drivers in mountainous areas of China. *Sci. Total Environ.* **2020**, *719*, 135132. [[CrossRef](#)] [[PubMed](#)]
13. Ou-Yang, X.; Zhu, X. Spatio-temporal characteristics of urban land expansion in Chinese urban agglomerations. *Acta Geogr. Sin.* **2020**, *75*, 571–588. (In Chinese with English Abstract)
14. Sun, H.; Wei, J.; Han, Q. Assessing land-use change and landscape connectivity under multiple green infrastructure conservation scenarios. *Ecol. Indic.* **2022**, *142*, 109236. [[CrossRef](#)]
15. Wang, Q.; Wang, H. Spatiotemporal dynamics and evolution relationships between land-use/land cover change and landscape pattern in response to rapid urban sprawl process: A case study in Wuhan, China. *Ecol. Eng.* **2022**, *182*, 106716. [[CrossRef](#)]
16. Deng, L.; Zhang, Q.; Cheng, Y.; Cao, Q.; Wang, Z.; Wu, Q.; Qiao, J. Underlying the influencing factors behind the heterogeneous change of urban landscape patterns since 1990: A multiple dimension analysis. *Ecol. Indic.* **2022**, *140*, 108967. [[CrossRef](#)]
17. Lambin, E.F.; Turner, B.L.; Geist, H.J.; Agbola, S.B.; Angelsen, A.; Bruce, J.W.; Coomes, O.T.; Dirzo, R.; Fischer, G.; Folke, C.; et al. The causes of land-use and land-cover change: Moving beyond the myths. *Glob. Environ. Chang.* **2001**, *11*, 261–269. [[CrossRef](#)]
18. Hassan, M.M. Monitoring land use/land cover change, urban growth dynamics and landscape pattern analysis in five fastest urbanized cities in Bangladesh. *Remote Sens. Appl. Soc. Environ.* **2017**, *7*, 69–83. [[CrossRef](#)]
19. Zhu, Q.Q.; Lei, Y.; Sun, X.L.; Guan, Q.F.; Zhong, Y.F.; Zhang, L.P.; Li, D.R. Knowledge-guided land pattern depiction for urban land use mapping: A case study of Chinese cities. *Remote Sens. Environ.* **2022**, *272*, 112916. [[CrossRef](#)]
20. Ouyang, X.; Tang, L.; Wei, X.; Li, Y. Spatial interaction between urbanization and ecosystem services in Chinese urban agglomerations. *Land Use Policy* **2021**, *109*, 105587. [[CrossRef](#)]
21. Xie, J.; Xie, B.; Zhou, K.; Li, J.; Xiao, J.; Liu, C. Impacts of landscape pattern on ecological network evolution in Changsha-Zhuzhou-Xiangtan Urban Agglomeration, China. *Ecol. Indic.* **2022**, *145*, 109716. [[CrossRef](#)]
22. Alphan, H.; Karamanli, E.; Derse, M.A.; Uslu, C. Analyzing pattern features of urban/rural residential land use change: The case of the southern coast of Turkey. *Land Use Policy* **2022**, *122*, 106348. [[CrossRef](#)]
23. Duan, X.; Chen, Y.; Wang, L.; Zheng, G.; Liang, T. The impact of land use and land cover changes on the landscape pattern and ecosystem service value in Sanjiangyuan region of the Qinghai-Tibet Plateau. *J. Environ. Manag.* **2023**, *325*, 116539. [[CrossRef](#)]
24. Chu, Y.F. A study on the evaluation of tourist areas in China. *Acta Geogr. Sin.* **1991**, *46*, 396–404, (In Chinese with English Abstract).
25. Guo, Y.; Jiang, J.B.; Li, S.C. A Sustainable Tourism Policy Research Review. *Sustainability* **2019**, *11*, 3187. [[CrossRef](#)]
26. Baloch, Q.B.; Shah, S.N.; Iqbal, N.; Sheeraz, M.; Asadullah, M.; Mahar, S.; Khan, A.U. Impact of tourism development upon environmental sustainability: A suggested framework for sustainable ecotourism. *Environ. Sci. Pollut. Res.* **2023**, *30*, 5917–5930. [[CrossRef](#)] [[PubMed](#)]
27. Fadafan, F.K.; Danehkar, A.; Pourebrahim, S. Developing a non-compensatory approach to identify suitable zones for intensive tourism in an environmentally sensitive landscape. *Ecol. Indic.* **2018**, *87*, 152–166. [[CrossRef](#)]
28. Schirpke, U.; Tappeiner, G.; Tasser, E.; Tappeiner, U. Using conjoint analysis to gain deeper insights into aesthetic landscape preferences. *Ecol. Indic.* **2019**, *96*, 202–212. [[CrossRef](#)]
29. Howard, R.A. Information value theory. *IEEE Trans. Syst. Sci. Cybern.* **1966**, *2*, 22–26. [[CrossRef](#)]
30. Bonham-Carter, G.F.; Agterberg, F.P.; Wright, D.F. Weights of evidence modeling: A new approach to mapping mineral potential. *Geol. Surv. Can.* **1989**, *89*, 171–183.
31. Cheng, E.; Li, H. Analytic hierarchy process. *Meas. Bus. Excell.* **1997**, *5*, 30–37. [[CrossRef](#)]
32. Masih, M.; Jozi, S.A.; Lahijanian, A.A.; Danehkar, A.; Vafaeinejad, A. Capability assessment and tourism development model verification of Haraz watershed using analytical hierarchy process (AHP). *Environ. Monit. Assess.* **2018**, *190*, 16. [[CrossRef](#)] [[PubMed](#)]
33. Deng, J.; Che, T.; Xiao, C.D.; Wang, S.J.; Dai, L.Y.; Meerzhan, A. Suitability analysis of ski areas in China: An integrated study based on natural and socioeconomic conditions. *Cryosphere* **2019**, *13*, 2149–2167. [[CrossRef](#)]
34. Adrianto, L.; Kurniawan, F.; Romadhon, A.; Bengen, D.G.; Sjafrie, N.D.M.; Damar, A.; Kleinertz, S. Assessing social-ecological system carrying capacity for urban small island tourism: The case of Tidung Islands, Jakarta Capital Province, Indonesia. *Ocean Coast. Manag.* **2021**, *212*, 12. [[CrossRef](#)]

35. Chaudhary, S.; Kumar, A.; Pramanik, M.; Negi, M.S. Land evaluation and sustainable development of ecotourism in the Garhwal Himalayan region using geospatial technology and analytical hierarchy process. *Environ. Dev. Sustain.* **2022**, *24*, 2225–2266. [[CrossRef](#)]
36. Cortes, C.; Vapnik, V. Support-vector networks. *Mach. Learn.* **1995**, *20*, 273–297. [[CrossRef](#)]
37. Breiman, L. Random forests. *Mach. Learn.* **2001**, *45*, 5–32. [[CrossRef](#)]
38. Friedman, J.H. Greedy function approximation: A gradient boosting machine. *Ann. Stat.* **2001**, *29*, 1189–1232. [[CrossRef](#)]
39. Cramer, J.S. The origins of logistic regression. *Tinbergen Inst. Discuss. Pap.* **2002**, *119*, 1–15. [[CrossRef](#)]
40. Lawrence, S.; Giles, C.L.; Tsoi, A.C.; Back, A.D. Face recognition: A convolutional neural network approach. *IEEE Trans. Neural Netw.* **1997**, *8*, 98–113. [[CrossRef](#)]
41. Mao, W.L.; Lu, D.B.; Hou, L.; Liu, X.; Yue, W.Z. Comparison of Machine-Learning Methods for Urban Land-Use Mapping in Hangzhou City, China. *Remote Sens.* **2020**, *12*, 2817. [[CrossRef](#)]
42. Talukdar, S.; Singha, P.; Mahato, S.; Shahfahad; Pal, S.; Liou, Y.A.; Rahman, A. Land-Use Land-Cover Classification by Machine Learning Classifiers for Satellite Observations—A Review. *Remote Sens.* **2020**, *12*, 1135. [[CrossRef](#)]
43. Abdi, A.M. Land cover and land use classification performance of machine learning algorithms in a boreal landscape using Sentinel-2 data. *GISci. Remote Sens.* **2020**, *57*, 1–20. [[CrossRef](#)]
44. Zhang, T.L.; Hou, M.Z.; Zhou, T.; Liu, Z.D.; Cheng, W.R.; Cheng, Y.J. Land-use classification via ensemble dropout information discriminative extreme learning machine based on deep convolution feature. *Comput. Sci. Inf. Syst.* **2020**, *17*, 427–443. [[CrossRef](#)]
45. Liang, J.; Xu, J.C.; Shen, H.F.; Fang, L. Land-use classification via constrained extreme learning classifier based on cascaded deep convolutional neural networks. *Eur. J. Remote Sens.* **2020**, *53*, 219–232. [[CrossRef](#)]
46. Reznik, T.; Chytry, J.; Trojanova, K. Machine Learning-Based Processing Proof-of-Concept Pipeline for Semi-Automatic Sentinel-2 Imagery Download, Cloudiness Filtering, Classifications, and Updates of Open Land Use/Land Cover Datasets. *ISPRS Int. J. Geo-Inf.* **2021**, *10*, 102. [[CrossRef](#)]
47. Xiang, J.; Xiao, K.Y.; Carranza, E.J.M.; Chen, J.P.; Li, S. 3D Mineral Prospectivity Mapping with Random Forests: A Case Study of Tongling, Anhui, China. *Nat. Resour. Res.* **2020**, *29*, 395–414. [[CrossRef](#)]
48. Qin, Y.Z.; Liu, L.M.; Wu, W.C. Machine Learning-Based 3D Modeling of Mineral Prospectivity Mapping in the Anqing Orefield, Eastern China. *Nat. Resour. Res.* **2021**, *30*, 3099–3120. [[CrossRef](#)]
49. Deng, H.; Zheng, Y.; Chen, J.; Yu, S.Y.; Xiao, K.Y.; Mao, X.C. Learning 3D mineral prospectivity from 3D geological models using convolutional neural networks: Application to a structure-controlled hydrothermal gold deposit. *Comput. Geosci.* **2022**, *161*, 105074. [[CrossRef](#)]
50. Zuo, R.G.; Xu, Y. Graph Deep Learning Model for Mapping Mineral Prospectivity. *Math. Geosci.* **2023**, *55*, 1–21. [[CrossRef](#)]
51. Nguyen, H.; Mehrabi, M.; Kalantar, B.; Moayed, H.; Abdullahi, M.M. Potential of hybrid evolutionary approaches for assessment of geo-hazard landslide susceptibility mapping. *Geomat. Nat. Hazards Risk* **2019**, *10*, 1667–1693. [[CrossRef](#)]
52. Zhang, Y.; Wu, W.; Qin, Y.; Lin, Z.; Zhang, G.; Chen, R.; Song, Y.; Lang, T.; Zhou, X.; Huangfu, W.; et al. Mapping Landslide Hazard Risk Using Random Forest Algorithm in Guixi, Jiangxi, China. *ISPRS Int. J. Geo-Inf.* **2020**, *9*, 695. [[CrossRef](#)]
53. Qin, Y.Z.; Cao, L.; Bolorani, A.D.; Wu, W.C. High-Resolution Mining-Induced Geo-Hazard Mapping Using Random Forest: A Case Study of Liaojaping Orefield, Central China. *Remote Sens.* **2021**, *13*, 3638. [[CrossRef](#)]
54. Zhou, X.T.; Wu, W.C.; Qin, Y.Z.; Fu, X. Geoinformation-based landslide susceptibility mapping in subtropical area. *Sci. Rep.* **2021**, *11*, 24325. [[CrossRef](#)] [[PubMed](#)]
55. Torre-Tojal, L.; Lopez-Guede, J.M.; Romay, M.M.G. Estimation of forest biomass from light detection and ranging data by using machine learning. *Expert Syst.* **2019**, *36*, 15. [[CrossRef](#)]
56. Mansaray, L.R.; Zhang, K.Y.; Kanu, A.S. Dry biomass estimation of paddy rice with Sentinel-1A satellite data using machine learning regression algorithms. *Comput. Electron. Agric.* **2020**, *176*, 9. [[CrossRef](#)]
57. Huang, X.; Wu, W.; Shen, T.; Xie, L.; Qin, Y.; Peng, S.; Zhou, X.; Fu, X.; Li, J.; Zhang, Z.; et al. Estimating Forest Canopy Cover by Multiscale Remote Sensing in Northeast Jiangxi, China. *Land* **2021**, *10*, 433. [[CrossRef](#)]
58. Sharma, P.; Leigh, L.; Chang, J.Y.; Maimaitijiang, M.; Caffe, M. Above-Ground Biomass Estimation in Oats Using UAV Remote Sensing and Machine Learning. *Sensors* **2022**, *22*, 601. [[CrossRef](#)]
59. Bolorani, A.D.; Samany, N.N.; Papi, R.; Soleimani, M. Dust source susceptibility mapping in Tigris and Euphrates basin using remotely sensed imagery. *Catena* **2022**, *209*, 105795. [[CrossRef](#)]
60. Papi, R.; Attarchi, S.; Bolorani, A.D.; Samany, N.N. Knowledge discovery of Middle East dust sources using Apriori spatial data mining algorithm. *Ecol. Inform.* **2022**, *72*, 101867. [[CrossRef](#)]
61. Van-der, L.; Rabe, S.; Held, A.; Jakimow, M.; Leitão, B.; Okujeni, P.J.; Schwieder, A.M.; Suess, S.; Hostert, P. The EnMAP-Box—A toolbox and application programming interface for EnMAP data processing. *Remote Sens.* **2015**, *7*, 11249–11266. [[CrossRef](#)]
62. Mcgarigal, K. *FRAGSTATS: Spatial Pattern Analysis Program for Quantifying Landscape Structure*; US Department of Agriculture, Forest Service, Pacific Northwest Research Station: Portland, OR, USA, 1995; pp. 1–132.
63. Raines, G.L. Description and comparison of geologic maps with FRAGSTATS—A spatial statistics program. *Comput. Geosci.* **2002**, *28*, 169–177. [[CrossRef](#)]
64. Quinlan, J.R. Induction of Decision Trees. *Mach. Learn.* **1986**, *1*, 81–106. [[CrossRef](#)]
65. Breiman, L. Bagging predictors. *Mach. Learn.* **1996**, *24*, 123–140. [[CrossRef](#)]
66. Loomis, J.M. Analysis of tactile and visual confusion matrices. *Percept. Psychophys.* **1982**, *31*, 41–52. [[CrossRef](#)]

67. Wu, J.G. Landscape Ecology—Concepts and Theories. *Chin. J. Ecol.* **2000**, *1*, 42–52. (In Chinese with English Abstract)
68. Li, X.; Lu, L.; Cheng, G.; Xiao, H. Quantifying landscape structure of the Heihe River Basin, north-west China using FRAGSTATS. *J. Arid. Environ.* **2001**, *48*, 521–535. [[CrossRef](#)]
69. Kaufman, Y.J.; Tanre, D. Atmospherically resistant vegetation index (ARVI) for eos-modis. *IEEE Trans. Geosci. Remote Sens.* **1992**, *30*, 261–270. [[CrossRef](#)]
70. Gao, B.C. NDWI—A normalized difference water index for remote sensing of vegetation liquid water from space. *Remote Sens. Environ.* **1996**, *58*, 257–266. [[CrossRef](#)]
71. Zhang, H.; Du, P.J.; Lu, J.Q.; Li, E.Z. Ecological change analysis of nanjing city based on remote sensing ecological index. *Geospat. Inf.* **2017**, *15*, 58–62 + 10. (In Chinese with English Abstract)
72. Li, B.L.; Ti, C.P.; Yan, X.Y. Study of derivation of tasseled cap transformation for landsat 8 oli images. *Sci. Surv. Mapp.* **2016**, *41*, 102–107. (In Chinese with English Abstract)
73. Yang, R.B. A new attempt to protect and use the former revolutionary residence site—On the site management of Ruijin Central Revolutionary Base Memorial. *Cult. Relics South. China* **2005**, *2*, 113–115. (In Chinese)
74. Jenks, G.F. The data model concept in statistical mapping. *Int. Yearb. Cartogr.* **1967**, *7*, 186–190.

Disclaimer/Publisher’s Note: The statements, opinions and data contained in all publications are solely those of the individual author(s) and contributor(s) and not of MDPI and/or the editor(s). MDPI and/or the editor(s) disclaim responsibility for any injury to people or property resulting from any ideas, methods, instructions or products referred to in the content.